Environ Monit Assess (2019) 191:364
https://doi.org/10.1007/s10661-019-7456-6

The environmental quality of sediments of rivers near prospection areas of semiprecious rocks

Paulo Roberto Bairros da Silva · Francisco Ernesto Dalla Nora · Rodrigo José de Castro · Arci Dirceu Wastowski · Frederico Fabio Mauad

Received: 7 November 2018 / Accepted: 4 April 2019

Abstract Mineral exploration areas are recognized for negatively affecting site environmental quality. The recent contaminations in the cities of Brumadinho, Mariana, Santo Antônio do Grama (Minas Gerais), and Barcarena (Pará) point to the seriousness of this issue in Brazil. However, studies on the influence of mining tailings from the extraction of semiprecious rocks on the quality of the sediments of water systems are rare. The aim of this study is to evaluate the influence of mining activities (amethyst, quartz, agate, calcite, and gypsum) on the quality of the sediments of Rio de Várzea, southern Brazil, the biggest region of amethyst rock extraction in the world. The concentrations of the chemical species Al_2O_3, SiO_2, P_2O_5, K_2O, CaO, TiO_2, Fe_2O_3, Cr, Mn, Co, Cu, Zn, Zr, Ba, Cd, and Pb were determined by the technique energy-dispersive X-ray emission spectrometry (EDXRF). In the study, moderate contamination of the sediments of the Várzea River was demonstrated by means of background strategies (contamination factor, enrichment factor, and geoaccumulation index). Statistical analysis with the use of ANOVA, Tukey test, and principal component analysis revealed significant differences of concentrations of the chemical species of the sediments at the exit of the mining zone in relation to the other study areas.

Keywords Sediments · Index of quality · Mining · Metals

Introduction

Mineral exploration activities tend to induce environmental impacts in the regions where they develop, and their wastes (solid waste not yet recoverable by technological and/or economically viable processes) are recognized by the contribution of potentially deleterious species to the water systems (Ayari et al. 2016; Paspacaud et al. 2015). In mining areas, the release of contaminants can occur through acid drainage of wastes, dam breakage, erosion, and surface runoff (Vosoogh et al. 2016; Fan et al. 2014).

The environmental risk in these regions is due to the concentrations of chemical species, such as metals and nutrients, present in the wastes normally stored in the open air, which can be fragmented and transported by rainwater, leading to the entry of these species into the water systems (Ontiveros-

Electronic supplementary material The online version of this article (https://doi.org/10.1007/s10661-019-7456-6) contains supplementary material, which is available to authorized users.

P. R. B. da Silva (✉) · F. F. Mauad
Center for Hydric Resources and Environmental Studies, São Carlos Engineering School, University of São Paulo, São Carlos, SP 13566-590, Brazil
e-mail: paulo_bairros@usp.br

F. E. D. Nora
Department of Agronomic and Environmental Sciences, UFSM - Frederico Westphalen Campus, University of Santa Maria, Frederico Westphalen, RS 98400-000, Brazil

R. J. de Castro · A. D. Wastowski
Department of Environmental Engineering and Technology, UFSM - Frederico Westphalen Campus, University of Santa Maria, Frederico Westphalen, RS 98400-000, Brazil

Published online: 14 May 2019

Cuadras et al. 2018; Vosoogh et al. 2016). These materials, when going into the aquatic environment, are associated with surface processes such as adsorption, complexation, and reprecipitation, and tend to decant, becoming part of the sediments (Remor et al. 2018; Sundararajan et al. 2017; Fan et al. 2014).

The contamination of sediments by chemical species such as metals and nutrients represents a threat to aquatic ecosystems due to their possible toxicity, persistence, bioavailability, bioaccumulation, and biomagnification in the food web (Silva et al. 2016; Pejman et al. 2015). In watersheds where mining activities take place, concentrations of chemical species in sediments are higher than the background levels and may pose risks as environmental stressors (Ontiveros-Cuadras et al. 2018; Vosoogh et al. 2016).

In this sense, the evaluation of the risks associated with the sediment quality by indexes that use the backgrounds of local concentrations of chemical species has been a widely used approach and a tool for the management of water resources (Silva et al. 2017a, b; Sundararajan et al. 2017; Maanan et al. 2015). The basis of the background method is the assumption that concentrations above background values cause adverse effects on ecosystems (Maanan et al. 2015; CCME 1995).

This approach is well suited for areas where there are no values indicative of sediment quality in the water systems, providing an adequate reference for environmental assessment (Remor et al. 2018; Vosoogh et al. 2016; CCME 1995). In this context, this study characterizes the influence of the mineral extraction activities (amethyst, quartz, agate, calcite, and gypsum) on the quality of the sediments of Várzea River, southern

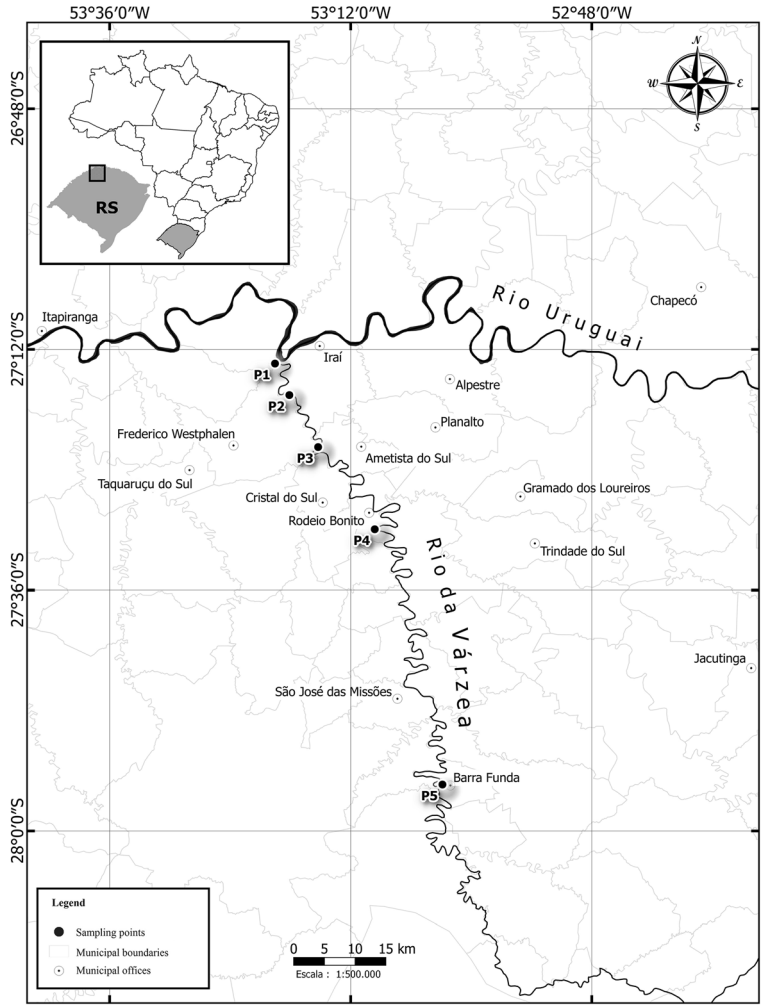

Fig. 1 Municipalities belonging to the mining region, collection points of the sediment samples, and spatial distribution of the course occupied by the Várzea River

Brazil, where the region of the greatest extraction of amethyst geodes of the world is located (Hartmann et al. 2017; Hartmann et al. 2015; Baggio et al. 2015).

Materials and methods

Study area and selection of sampling points

The watershed of Várzea River is located in the north of Rio Grande do Sul State, covering 55 municipalities with a drainage area of 9324 km^2 and a population of 328,057 inhabitants. The main water body component is the Várzea River, which is approximately 165 km long (State Foundation for Environmental Protection (FEPAM) 2018, Secretary of Environment and Sustainable Development (SEMA) 2012). Figure 1 highlights the Várzea River and locates the sampling points.

In the northern part of the river basin, mining activities in horizontal underground mining are observed in the municipalities of Ametista do Sul, Frederico Westphalen, Rodeio Bonito, Cristal do Sul, Planalto, Iraí, Trindade do Sul, and Gramado dos Loureiros (Hartmann et al. 2017; Baggio et al. 2015). Currently, there are 500 mines (active and inactive), most them in Ametista do Sul, the municipality that is the largest amethyst producer in the world (Hartmann et al. 2017; Rosenstengel and Hartmann 2012).

The area is characterized by geological faults and successive volcanic spills that occurred in the region; however, the event that originated the basalts of interest for mineral exploration was influenced by hydrothermal character alterations due to a connection with the Guarani Aquifer (Gadens-Marcon et al. 2004). The monthly extraction in the areas varies around 600 gross tons of semiprecious rocks (quartz, agate, amethysts, calcite, and gypsum); about 80% of the rocks are destined for markets in China, Taiwan, Hong Kong, Thailand, the USA, Germany, Spain, and Italy, moving around R $ 30 million only in 2018 (Folha do Noroeste 2019; Hartmann et al. 2017; Rosenstengel and Hartmann 2012).

The activity generates as environmental liabilities basalt rock tailings (rock of volcanic origin rich in iron and magnesium silicates), normally stored in the open (Hartmann et al. 2017; Pinto and Hartmann 2011; Branco 2002). Figure 2 shows the spatial location of the mines in the municipality of Ametista do Sul.

The basaltic rejects tend to change and can decompose under favorable conditions in 10 months (Baggio et al. 2015; Branco 2002). It is believed that the wastes stored on the slopes of the mineral extraction areas can alter the water system influencing the quality of the sediments of the Várzea River. Figure 3 highlights (a) the accumulation of wastes in front of mines in the municipality of Ametista do Sul, RS; (b) the details of

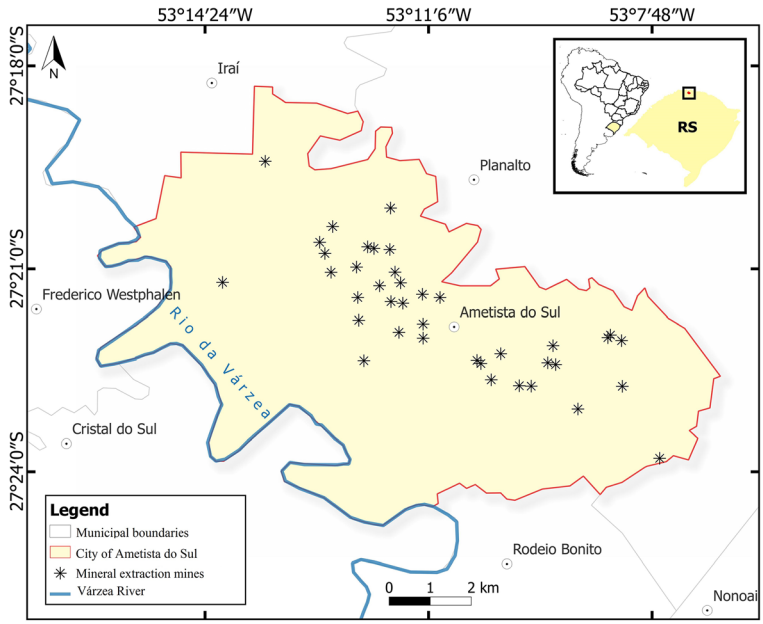

Fig. 2 Zones of mineral extraction in the municipality of Ametista do Sul and the Várzea River

Fig. 3 **a** Mining rejects accumulated in a mining zone in the municipality of Ametista do Sul; **b** different stages of fragmentation of basalt wastes in open air in the municipality of Ametista do Sul, southern Brazil

the basalt wastes in several states of decomposition in a mine in the municipality of Ametista do Sul, RS.

Studies have been conducted to characterize the concentrations of the elements present in the wastes in order to determine the formation and extent of the effluent that gave rise to the region and the gems (Baggio et al. 2015; Hartmman et al. 2015; Rosenstengel e Hartmann 2012; Pinto e Hartmann 2011). However, none sought to evaluate the influence of mineral extraction activities on sediment quality. Table 1 shows the mean concentration of chemical species present in the basalt rejects of the region.

The predominant soil in this hydrographic basin is the humid dystrophic red latosol (of strong acidity,

Table 1 Mean concentrations of chemical species in basalts of the Serra Geral group

	Studies developed in the mining zone			
	Pinto and Hartmann (2011) (Frederico Westphalen-Iraí)	Rosestengel and Hartmann (2012) (Ametista-Rio da Várzea)	Baggio et al. (2015) (Ametista-Parque museu)	Hartmman et al. (2015) (COOGAMAI)
Oxides (%)				
Al_2O_3	12.6	12.9	12.9	14.8
SiO_2	50.3	48.8	48.5	48.1
P_2O_5	0.3	0.3	0.3	3.7
K_2O	1.3	1.0	1.2	1.3
CaO	8.6	9.5	9.6	8.3
TiO_2	2.5	2.5	2.3	12.5
Fe_2O_3	15.7	14.9	15.5	0.2
Elements ($\mu g\ g^{-1}$)				
Cr	*	*	*	*
Mn	*	*	*	*
Co	43.2	43.7	44.0	34.6
Cu	237.5	*	219.7	150.3
Zn	*	*	71.7	*
Zr	167.8	162.2	150.2	226.5
Cd	*	*	*	*
Ba	310.1	358.7	321.2	471.2
Pb	*	*	1.6	*

*Chemical species not characterized in the study

Table 2 Sediment contamination rank for evaluation by environmental quality indices

Value	Geoaccumulation index	Value	Enrichment factor	Value	Contamination factor
≤ 0	Unpolluted	< 1	Minimal enrichment limit	< 1	Low contamination
0–1	Unpolluted/moderately polluted	2–5	Moderate enrichment	1–3	Moderate contamination
1–2	Moderately polluted	5–20	Significant enrichment	3–6	Considerable contamination
2–3	Moderately/heavily polluted	20–40	Very highly enriched	≥ 6	Very high contamination
3–4	Heavily polluted	> 40	Extremely enriched		
4–5	Heavily/extremely polluted				
≥ 5	Extremely polluted				

advanced weathering, low nutrient reserve, reddish color, and clay texture, and which needs corrections in its fertility and fertilization), where crops such as wheat, maize, and soybean grow (MSRS 2019; EMBRAPA 2013; Kämpf and Streck 2010).

Sampling, packaging, and preparation of samples

Soil and sediment sampling procedures followed clean technique protocols (National Water Agency (ANA) & Environmental Company of São Paulo State (Cetesb), 2011; Filizola et al. 2006). Bottom sediment collection was performed with a stainless steel Petersen dredge (3 kg), and the procedures respected the representativeness of the region, with sampling in the cross section of the river (margins and center) forming a composite sample representative of the point.

Soil samples from the riparian forests were made by cleaning the surface with a stainless steel hoe and Dutch auger to 20 cm of depth (four samples, on the right bank and on the left bank) with a distance exceeding 50 m (upstream and downstream of the sediment sampling site) at the river bank.

The samples were stored in double polypropylene bags (2 L) of the Ziplock type, identified, and sent to the laboratory in cooling boxes for analysis. At the laboratory, the sediment samples were homogenized in clean trays with the aid of spatulas, both of polypropylene, and routed for drying in a circulation oven at 50 °C for 48 h.

The samples were disaggregated in agate mortar and separated into fine granulometric fractions (< 63 μm) for analysis of the chemical species. In this study, the results (in quintuplicates) of three sampling campaigns carried out between July 2016 and January 2017 were presented, comprising 15 samples composed of sediments (75 analyses) and 5 samples composed of soils (25 analyses).

Analytical method and determination of mean concentrations of chemical species

Table 3 Characterization of the EDXRF analytical process using certified reference material

	MRC ($\bar{x}$ + CI)	Determined ($\bar{x}$ + CI)	CV (%)	*R* (%)
Oxides (%)				
Al_2O_3	6.5 ± 0.2	6.4 ± 0.1	4.5	97.5
SiO_2	28.2 ± 0.2	27.3 ± 0.4	4.1	96.6
P_2O_5	0.33 ± 0.07	0.33 ± 0.01	3.1	99.1
K_2O	1.6 ± 0.1	1.6 ± 0.03	5.0	96.7
CaO	8.4 ± 0.2	8.1 ± 0.1	4.7	96.1
TiO_2	0.2 ± 0.02	0.2 ± 0.05	5.2	95.8
Fe_2O_3	3.0 ± 0.1	2.9 ± 0.5	4.5	96.1
Elements (μg g^{-1})				
Cr	30.0 ± 5	28.1 ± 1.16	11.3	95.4
Mn	267.0 ± 34	261.5 ± 3.0	3.3	97.9
Co	12.0 ± 1.5	12.7 ± 0.1	2.4	105.7
Cu	66.0 ± 9.0	66.7 ± 0.9	3.7	101.1
Zn	74.0 ± 9.0	70.2 ± 1.0	4.0	94.8
Zr	53.0	53.1 ± 0.4	2.2	100.2
Cd	0.9	1.3 ± 0.1	16.7	105.4
Ba	290.0 ± 40.0	285.6 ± 1.8	1.8	98.5
Pb	38.0 ± 4.0	36.5 ± 1.3	9.9	96.0

$\bar{x}$ mean concentration, *CI* confidence interval, *CV (%)* coefficient of variation, *R (%)* recovery, *MRC* reference material

Energy-dispersive X-ray emission spectroscopy (EDXRF) is a simultaneous, non-destructive, simplified preparation technique that has been employed in the quantification of species in environmental samples (Ontiveros-Cuadras et al. 2018; Ryan et al. 2017, Silva et al. 2016, Kontos et al. 2016). The EDXRF performance was evaluated by retrieving the Green River Shale (SGR-1b) certified sample from the United States Geological Survey with the safety of 30 data collection.

The analyses were performed on a Shimadzu equipment (model EDX-720), under the following conditions: Rh X-ray tube 3.0 kW; excitation of 15 kV for Si Ka and 50 kV for ULα; 10 mm collimator; Si (Li) detector cooled with liquid nitrogen; and integration time of 100 s. Measurements on samples (mass of 2 g) were supported (31 mm Closed X-Cell - SPEX) using thin film (*Mylar*®, 6.0 μm SPEX).

Sediment environmental quality indexes

The sediments are a complex mixture resulting from the transport of the eroded particles of the different component soils of a watershed, reflecting all the interactions that occur in the surface (Silva et al. 2016; Esteves and Camargo 2011). In this sense, the soil uses of the river basin itself have been a very useful strategy when local quality references to the sediments are not available (Sundararajan et al. 2017; Fan et al. 2014, CCME 1995).

The basis of the background method is the assumption that concentrations above background values cause adverse effects on ecosystems (Maanan et al. 2015, Matschullat et al. 2000, CCME 1995). Based on background strategies in relation to the presence of chemical species, quality indices were established from samples of soils obtained under the same conditions and in areas

Table 4 Concentrations in samples composed of soils collected in the riparian forest of Várzea River

	Barra Funda		Rodeio Bonito		Ametista		Iraí-Ponte Velha		Iraí-BR 386	
	$\bar{x} \pm$ CI	CV (%)	$\bar{x} \pm$ IC	CV (%)	$\bar{x} \pm$ IC	CV (%)	$\bar{x} \pm$ IC	CV (%)	$\bar{x} \pm$ CI	CV (%)
Oxides (%)										
Al_2O_3	17.0 ± 0.1	0.5	12.9 ± 0.4	3.2	13.4 ± 0.4	3.7	12.7 ± 0.7	5.5	15.2 ± 0.5	3.5
SiO_2	26.6 ± 0.1	0.4	30.2 ± 0.9	3.2	29.7 ± 0.5	1.6	27.8 ± 1.2	4.3	31.1 ± 1.3	4.8
P_2O_5	0.3 ± 0.01	4.1	0.3 ± 0.01	5.1	0.3 ± 0.01	5.5	0.3 ± 0.01	1.1	0.3 ± 0.01	4.6
K_2O	0.2 ± 0.01	3.0	0.4 ± 0.01	1.1	0.4 ± 0.01	1.4	0.3 ± 0.01	3.0	0.4 ± 0.01	4.3
CaO	0.7 ± 0.01	1.8	1.1 ± 0.01	1.0	1.2 ± 0.02	1.5	0.9 ± 0.02	2.7	1.0 ± 0.03	3.9
TiO_2	6.3 ± 0.1	2.4	7.7 ± 0.6	9.5	7.0 ± 0.4	6.2	6.3 ± 0.2	3.2	5.4 ± 0.2	3.5
Fe_2O_3	19.5 ± 0.5	2.8	16.6 ± 0.2	1.7	16.4 ± 0.2	1.2	16.8 ± 0.5	3.2	17.3 ± 0.5	3.3
Elements (μg g^{-1})										
Cr	93.0 ± 11.0	13.4	80.1 ± 9.7	13.8	75.2 ± 11.5	17.4	79.0 ± 11.1	14.4	83.0 ± 11.4	15.6
Mn	2201.8 ± 61.5	3.2	2640.9 ± 108.3	4.7	2310.8 ± 11.5	0.6	2739.3 ± 90.3	3.4	3184.0 ± 96.1	3.4
Co	69.3 ± 2.0	3.3	59.4 ± 1.7	3.3	60.3 ± 0.7	1.3	61.1 ± 2.4	4.1	62.5 ± 1.4	2.5
Cu	147.6 ± 5.1	3.9	88.6 ± 9.2	11.9	97.5 ± 1.7	2.0	97.8 ± 7.1	7.4	98.3 ± 4.0	4.7
Zn	78.9 ± 5.3	7.7	77.4 ± 5.4	7.9	76.8 ± 4.7	6.9	76.9 ± 7.8	10.4	80.3 ± 5.7	8.0
Zr	132.9 ± 5.2	4.5	132.3 ± 3.6	3.1	126.6 ± 7.7	6.9	125.4 ± 6.2	5.1	133.6 ± 6.8	5.7
Cd	2.0 ± 0.2	9.4	2.3 ± 0.2	8.3	2.2 ± 0.2	12.1	1.9 ± 0.1	6.8	2.2 ± 0.2	9.6
Ba	7055.4 ± 166.2	2.7	8863.6 ± 791.9	10.2	7962.7 ± 413.2	5.9	7234.0 ± 248.0	3.5	6205.2 ± 191.3	3.5
Pb	60.1 ± 12.2	23.2	49.2 ± 5.4	12.5	44.5 ± 2.7	6.8	45.7 ± 3.8	8.4	52.9 ± 5.0	10.7

$\bar{x}$ mean concentrations, *CI* confidence interval

Table 5 Mean concentrations of the Várzea River sediment samples for the sampling points

	Analyte	BF		RB		A		IPV		IBR	
		$(\overline{X} \pm IC)$	CV (%)	$(\overline{X} \pm CI)$	CV (%)	$(\overline{X} \pm CI$	CV (%)	$(\overline{X} \pm CI)$	CV (%)	$(\overline{X} \pm CI)$	CV (%)
1st sampling campaign	Al_2O_3	14.9 ± 1.8	14.1	13.4 ± 0.4	3.4	13.6 ± 0.4	3.0	12.5 ± 0.2	2.1	15.2 ± 1.4	10.2
	SiO_2	26.6 ± 3.6	15.6	31.7 ± 1.3	4.6	31.2 ± 0.7	2.5	32.6 ± 0.4	1.3	30.0 ± 2.5	9.7
	P_2O_5	0.3 ± 0.04	17.2	0.3 ± 0.01	4.0	0.3 ± 0.01	3.9	0.3 ± 0.01	3.8	0.3 ± 0.02	7.2
	K_2O	0.2 ± 0.03	16.2	0.4 ± 0.01	4.3	0.4 ± 0.01	1.7	0.4 ± 0.1	3.19	0.4 ± 0.03	9.4
	CaO	0.8 ± 0.1	19.2	1.1 ± 0.04	4.2	1.1 ± 0.03	2.7	1.0 ± 0.02	2.1	0.9 ± 0.07	9.1
	TiO_2	6.8 ± 1.2	20.2	8.6 ± 0.3	3.9	7.5 ± 0.3	4.8	6.2 ± 0.2	2.9	4.4 ± 0.4	9.9
	Fe_2O_3	16.8 ± 2.6	17.5	17.0 ± 0.5	3.7	17.0 ± 0.3	1.9	16.0 ± 0.3	1.9	17.0 ± 1.4	9.2
	Cr	95.0 ± 8.5	10.2	72.5 ± 10.2	16.1	71.3 ± 14.0	22.4	71.4 ± 9.1	14.6	83.2 ± 7.9	10.8
	Mn	2196.6 ± 71.7	3.7	2172.7 ± 129.	6.8	2006.3 ± 304.5	17.3	2336.0 ± 291.5	14.2	3042.7 ± 231.0	8.7
	Co	56.7 ± 1.7	3.4	51.3 ± 3.4	7.5	49.6 ± 7.7	17.7	43.9 ± 5.0	12.9	48.8 ± 3.7	8.6
	Cu	105.6 ± 5.4	5.8	90.8 ± 9.3	11.7	101.3 ± 2.8	3.1	122.4 ± 21.5	20.0	97.7 ± 4.2	4.9
	Zn	84.01 ± 5.5	7.5	80.7 ± 12.1	17.1	73.7 ± 1.8	2.9	135.5 ± 23.4	19.7	76.9 ± 5.4	8.0
	Zr	134.8 ± 5.1	4.4	134.7 ± 11.2	9.5	131.0 ± 7.3	6.4	112.7 ± 16.3	16.5	123.2 ± 11.8	10.9
	Cd	2.1 ± 0.3	14.4	2.1 ± 0.4	23.2	2.1 ± 0.5	29.6	2 ± 0.5	30.8	2.2 ± 0.2	8.1
	Ba	7978.9 ± 244.6	3.5	9707.1 ± 380.8	4.5	8471.5 ± 358.0	4.2	7017.9 ± 753.1	12.2	4057.3 ± 279.2	6.4
	Pb	52.5 ± 5.7	12.3	49.8 ± 5.4	12.3	46.5 ± 10.1	24.9	33.2 ± 10.0	34.4	38.1 ± 6.1	18.2
2nd sampling campaign	Al_2O_3	15.6 ± 0.4	3.0	13.1 ± 1.0	8.7	13.6 ± 0.4	3.1	6.8 ± 0.7	12.1	12.9 ± 0.7	5.8
	SiO_2	29.7 ± 0.7	2.7	31.4 ± 2.1	7.7	31.8 ± 0.8	2.7	16.0 ± 1.4	10.2	24.3 ± 0.9	4.5
	P_2O_5	0.3 ± 0.01	3.7	0.3 ± 0.02	7.7	0.3 ± 0.01	3.1	0.3 ± 0.01	5.1	0.3 ± 0.02	6.2
	K_2O	0.3 ± 0.01	2.6	0.3 ± 0.02	8.5	0.3 ± 0.01	3.0	0.2 ± 0.02	13.7	0.3 ± 0.02	7.1
	CaO	0.8 ± 0.01	1.0	0.8 ± 0.06	8.2	0.8 ± 0.03	3.8	0.7 ± 0.1	14.4	0.8 ± 0.03	4.8
	TiO_2	6.6 ± 0.05	0.8	5.9 ± 0.4	7.5	6.6 ± 0.2	3.7	19.0 ± 2.9	17.1	4.8 ± 0.2	5.3
	Fe_2O_3	18.3 ± 0.1	0.6	16.3 ± 1.1	8.0	17.4 ± 0.7	3.8	17.4 ± 0.8	5.5	17.7 ± 0.2	1.3
	Cr	98.5 ± 14.7	17.0	82.4 ± 16.8	23.3	87.1 ± 8.2	10.8	93.1 ± 14.1	17.3	84.5 ± 7.3	9.8
	Mn	1864.5 ± 132.9	8.1	2593.3 ± 200.5	9.7	2651.0 ± 52.3	2.2	2119.0 ± 129.0	6.9	2767.7 ± 150.7	6.2
	Co	60.0 ± 5.0	9.4	56.3 ± 4.6	9.4	60.1 ± 1.0	2.0	55.8 ± 3.6	7.4	55.4 ± 2.6	5.3
	Cu	104.5 ± 8.3	9.1	89.5 ± 9.2	11.7	104.4 ± 2.8	3.1	65.3 ± 6.3	10.9	96.7 ± 4.4	5.2
	Zn	74.1 ± 7.4	11.3	76.6 ± 6.1	9.1	78.3 ± 5.7	8.4	73.0 ± 2.5	3.9	75.8 ± 3.4	5.1
	Zr	129.2 ± 14.0	12.4	125.0 ± 13.9	12.7	138.8 ± 3.3	2.7	85.0 ± 3.4	4.6	121.5 ± 8.1	7.6
	Cd	2.0 ± 0.4	21.5	2.0 ± 0.6	30.3	2.0 ± 0.3	18.7	1.9 ± 0.2	10.8	1.8 ± 0.3	21.3

Table 5 (continued)

	Analyte	BF		RB		A		IPV		IBR	
		$(\overline{X} \pm \mathrm{IC})$	CV (%)	$(\overline{X} \pm \mathrm{CI})$	CV (%)	$(\overline{X} \pm \mathrm{CI}$	CV (%)	$(\overline{X} \pm \mathrm{CI})$	CV (%)	$(\overline{X} \pm \mathrm{CI})$	CV (%)
	Ba	7174.1 ± 484.9	7.7	6670.4 ± 523.5	8.9	7481.6 ± 136.7	2.1	21,450.5 ± 3550.6	18.9	5450.8 ± 241.6	5.1
	Pb	47.4 ± 7.9	18.9	44.3 ± 5.7	14.7	40.9 ± 3.6	10.1	39.6 ± 10.3	29.8	37.7 ± 2.4	7.3
3rd sampling campaign	Al_2O_3	14.4 ± 0.6	4.8	13.8 ± 0.3	2.1	13.8 ± 0.6	4.8	12.6 ± 0.05	0.4	14.3 ± 0.9	6.8
	SiO_2	30.0 ± 0.6	2.3	31.9 ± 0.5	1.9	29.7 ± 1.3	4.3	32.1 ± 0.9	3.0	31.4 ± 0.9	3.4
	P_2O_5	0.3 ± 0.01	3.6	0.3 ± 0.01	2.4	0.3 ± 0.01	2.0	0.3 ± 0.01	3.0	0.3 ± 0.01	2.9
	K_2O	0.3 ± 0.01	2.7	0.4 ± 0.01	3.2	0.3 ± 0.01	3.6	0.4 ± 0.01	3.7	0.3 ± 0.02	6.3
	CaO	0.9 ± 0.03	4.2	1.2 ± 0.02	1.5	0.9 ± 0.02	2.7	1.0 ± 0.03	2.8	0.9 ± 0.05	6.8
	TiO_2	6.8 ± 0.5	9.2	7.6 ± 0.2	2.3	6.3 ± 0.3	4.2	8.2 ± 0.4	4.8	7.0 ± 0.7	11.3
	Fe_2O_3	17.4 ± 0.4	2.7	16.9 ± 0.1	0.7	17.2 ± 0.6	3.45	17.0 ± 0.2	1.2	17.7 ± 0.4	2.4
	Cr	88.8 ± 7.0	9.0	85.4 ± 6.3	8.4	87.4 ± 9.0	11.7	80.5 ± 7.6	9.6	87.3 ± 4.3	5.6
	Mn	2351.2 ± 58.4	2.8	2278.9 ± 24.1	1.2	2419.4 ± 88.1	4.1	2660.3 ± 18.4	0.7	2582.2 ± 83.5	3.7
	Co	72.1 ± 1.4	2.3	70.4 ± 0.3	0.5	71.9 ± 2.6	4.1	69.3 ± 1.0	1.4	70.5 ± 2.4	3.8
	Cu	112.1 ± 2.3	2.3	101.2 ± 3.1	3.5	97.4 ± 4.7	5.5	106.0 ± 2.4	2.3	99.3 ± 7.9	9.0
	Zn	82.1 ± 1.9	2.7	79.7 ± 2.5	3.7	76.0 ± 3.4	5.2	81.2 ± 3.0	3.7	75.8 ± 4.3	6.5
	Zr	140.1 ± 11.0	8.9	136.0 ± 1.7	1.4	131.6 ± 4.5	3.9	137.5 ± 3.1	2.3	133.3 ± 5.8	4.9
	Cd	2.1 ± 0.3	17.1	2.3 ± 0.2	10.1	2.2 ± 0.1	6.1	2.3 ± 0.4	17.0	2.5 ± 0.1	5.0
	Ba	7683.3 ± 605.2	9.0	8775.3 ± 152.0	2.0	7121.5 ± 275.0	4.4	9382.5 ± 471.1	5.1	7416.4 ± 191.1	2.9
	Pb	67.2 ± 8.7	14.8	54.7 ± 3.9	8.2	55.0 ± 1.9	3.8	52.4 ± 0.7	1.4	49.2 ± 9.5	21.9

$\overline{x}$ mean concentrations of chemical species, *IC* confidence interval, *BF* Barra Funda, *RB* Rodeio Bonito, *A* Ametista, *IPV* Iraí-Ponte Velha, *IBR* Iraí-BR 386

Table 6 ANOVA: sediment samples from the Várzea River

Analyte	Sources of variation	SS	DF	MS	*F*	*p* value
Al_2O_3	Between groups	173.9	4	43.5	17.5	7.8×10^{-10}
	Within groups	163.9	66	2.5		
	Total	337.8	70			
SiO_2	Between groups	267	4	66.7	3.8	7.9×10^{-3}
	Within groups	1185.9	67	17.7		
	Total	1452.9	71			
P_2O_5	Between groups	0.003	4	0.0006	2.1	9.0×10^{-2}
	Within groups	0.02	67	0.0003		
	Total	0.023	71			
K_2O	Between groups	0.1	4	0.03	8.2	1.9×10^{-5}
	Within groups	0.2	67	0.003		
	Total	0.3	71			
CaO	Between groups	0.3	4	0.08	5.1	1.1×10^{-3}
	Within groups	1.1	67	0.02		
	Total	1.4	71			
TiO_2	Between groups	324.7	4	81.2	10.4	1.3×10^{-6}
	Within groups	523.5	67	7.8		
	Total	848.2	71			
Fe_2O_3	Between groups	6.5	4	1.6	1.4	2.0×10^{-1}
	Within groups	74.3	66	1.1		
	Total	80.8	70			
Cr	Between groups	1871.9	4	468.0	2.9	3.0×10^{-2}
	Within groups	1094.7	69	158.7		
	Total	12,819.8	73			
Mn	Between groups	3.5×10^6	4	875,782	11.3	4.0×10^{-7}
	Within groups	5.3×10^6	69	77,299.8		
	Total	8.8×10^6	73			
Co	Between groups	450.6	4	112.6	1.2	3.0×10^{-1}
	Within groups	6572.5	69	95.2		
	Total	7023.1	73			
Cu	Between groups	1557.4	4	389.3	1.9	1.0×10^{-1}
	Within groups	14,098.5	68	207.3		
	Total	15,655.9	72			
Zn	Between groups	4610.0	4	1152.5	4.7	2.0×10^{-3}
	Within groups	15,592.3	68	244.0		
	Total	21,202.3	72			
Zr	Between groups	4865.8	4	1216.4	6.1	3.0×10^{-3}
	Within groups	13,317.1	67	198.8		
	Total	18,182.8	71			
Cd	Between groups	0.1	4	0.02	0.1	1.0×10^0
	Within groups	11.4	69	0.2		
	Total	11.5	73			
Ba	Between groups	3.8×10^8	4	9.5×10^7	9.0	6.7×10^{-6}
	Within groups	7.3×10^8	69	1.0×10^7		

Table 6 (continued)

Analyte	Sources of variation	SS	DF	MS	*F*	*p* value
	Total	1.1×10^9	73			
Pb	Between groups	2050.6	4	512.6	5.0	1.4×10^{-3}
	Within groups	7125.3	69	103.3		
	Total	9175.9	73			

SS sum of squares, *DF* degrees of freedom, *MS* mean square, *F* Fisher's value

close to study points in the riparian forest (Sundararajan et al. 2017; Fan et al. 2014).

The use of environmental quality indices in the evaluation of sediment quality has been a widely used approach as a tool for the management of water resources (Lone et al. 2018; Sundararajan et al. 2017 and Maanan et al. 2015). Ciliary forests protect river banks due to their physical retention capacity and usually present soils with no horizons defined by the constant deposition of particles (Periotto and Cielo Filho 2014).

Thus, the use of soil chemical concentrations of ciliary forests for background strategies should be taken as a guideline rather than as a marker of sediment quality, since these tend to underestimate the significance of contamination levels (Silva et al. 2017a, b, CCME 1995). A number of geochemical techniques have been employed in an attempt to differentiate the natural concentrations of potentially pollutant concentrations in sediments. In this sense, this study determines the indices of contamination factor, enrichment factor, and geoaccumulation index (Lone et al. 2018; Silva et al. 2017b; Sundararajan et al. 2017).

The contamination of sediments can be expressed by the contamination factor (CF), expressed in the equation below, and allows individually evaluating the contamination of the sediments for a given individual chemical species:

$$\mathrm{CF} = \frac{C_\mathrm{m}}{B} \tag{1}$$

where C_m is the mean concentration determined in the sediment samples and B is the mean concentration value of a representative baseline for the study site (Remor et al. 2018; Sundararajan et al. 2017; Pejman et al. al. 2015). The enrichment factor (FE) indicates possible anthropogenic contributions of an individual chemical species by the double rationalization of the concentrations determined in the sediments and the local background value, and its values are expressed by the following equation:

$$\mathrm{EF} = \frac{(C_\mathrm{x}/C_\mathrm{ref})_\mathrm{sediment}}{(C_\mathrm{x}/C_\mathrm{ref})_\mathrm{background}} \tag{2}$$

where C_x is the concentration of the element in the sample and C_ref is the concentration of the reference element in the sediment. The reference element must have low concentration variability in the matrix; it is common to use concentrations of the chemical species Al, Mn, and Sr for this purpose (Lone et al. 2018; Remor et al. 2018).

In this study, the mineral oxide Fe_2O_3 was used as a normalizing element because it showed high abundance and low variability of concentrations between the sample points (see Tukey's test in Table 7) in the samples of local soils (Hanif et al. 2016; Pejman et al. 2015). FE values higher than 1 are associated with the contribution of chemical species in the water system (Herath et al. 2018; Sundararajan et al. 2017). The geoaccumulation index (I_Geo) performs a logarithmic normalization process of concentrations and indicates the level of contamination for sediments; the values are defined by the following equation:

$$I_\mathrm{Geo} = \log_2\left(\frac{C_n}{1.5 \times B_n}\right) \tag{3}$$

where C_n is the concentration in the sediment samples, B_n is the background concentration, and factor 1.5 is the background correction factor of the matrix (Sundararajan et al. 2017). To each quality index is associated a score that allows classifying the deleterious influence existing (Pejman et al. 2015). These classifications for the quality indexes enrichment factor, contamination factor, and geochemical index are presented in Table 2.

Statistical methods

The Kolmogorov-Smirnov test, ANOVA, Tukey test, and principal component analysis (PCA) were

Table 7 Tukey test of concentrations of chemical species in the sediments

Al_2O_3	BF	RB	A	IPV	IBR	SiO_2	BF	RB	A	IPV	IBR
BF		0.1	0.2	3.6×10^{-10}*	0.6	BF		0.3	0.7	0.4	1.0
RB	3.7		1.0	8.1×10^{-6}*	0.8	RB	2.7		1.0	6.7×10^{-3}*	0.3
A	3.1	0.6		2.6×10^{-6}*	0.9	A	1.9	0.7		3.3×10^{-2}*	0.6
IPV	11.2	8.0	8.1		1.5×10^{-7}*	IPV	2.4	5.0	4.2		0.5
IBR	2.1	1.6	1.0	9.2		IBR	0.1	2.8	2.0	2.2	
P_2O_5	BF	RB	A	IPV	IBR	K_2O	BF	RB	A	IPV	IBR
BF		0.7	0.2	0.6	6.0×10^{-2}	BF		2.5×10^{-5}*	3.5×10^{-4}*	0.2	3.7×10^{-3}*
RB	1.8		0.9	1.0	0.6	RB	7.3		1.0	0.07	0.6
A	3.0	1.3		1.0	1.0	A	6.2	0.9		0.3	0.9
IPV	2.1	0.4	0.9		0.8	IPV	3.2	3.8	2.9		0.6
IBR	3.9	2.1	0.8	1.6		IBR	5.2	2.0	1.1	1.9	
CaO	BF	RB	A	IPV	IBR	TiO_2	BF	RB	A	IPV	IBR
BF		3.7×10^{-3}*	0.1	0.9	1.0	BF		1.0	1.0	8.2×10^{-5}*	0.7
RB	5.3		0.7	7.3×10^{-2}	4.8×10^{-3}*	RB	0.9		1.0	7.8×10^{-4}*	0.3
A	3.4	1.7		0.6	0.1	A	0.1	0.8		1.4×10^{-4}*	0.7
IPV	1.3	3.7	2.0		0.9	IPV	6.8	5.9	6.6		7.1×10^{-7}
IBR	0.1	5.1	3.3	1.2		IBR	1.8	2.7	1.9	8.6	
Fe_2O_3	BF	RB	A	IPV	IBR	Cr	BF	RB	A	IPV	IBR
BF		0.3	1.0	0.6	1.0	BF		2.6×10^{-2}*	0.08	0.07	0.3
RB	2.7		0.7	1.0	0.3	RB	4.3		1.0	1.0	0.8
A	1.0	1.7		0.9	1.0	A	3.7	0.6		1.0	1.0
IPV	2.0	0.6	1.1		0.6	IPV	3.7	0.5	0.1		0.9
IBR	1.6×10^{-2}	2.7	0.9	2.0		IBR	2.8	1.5	0.9	1.0	
Mn	BF	RB	A	IPV	IBR	Co	BF	RB	A	IPV	IBR
BF		0.2	0.2	0.2	1.0×10^{-7}*	BF		0.8	0.9	0.2	0.7
RB	2.9		1.0	1.0	3.3×10^{-4}*	RB	1.4		1.0	0.8	1.0
A	3.1	0.1		1.0	4.8×10^{-4}*	A	1.0	0.5		0.6	1.0
IPV	2.9	0.04	0.1		4.8×10^{-4}*	IPV	2.9	1.5	2.0		0.9
IBR	9.1	6.3	6.1	6.1		IBR	1.8	0.4	0.9	1.1	
Cu	BF	RB	A	IPV	IBR	Zn	BF	RB	A	IPV	IBR
BF		0.08	0.8	0.3	0.4	BF		1.0	1.0	2.7×10^{-2}*	1.0
RB	3.6		0.6	1.0	0.9	RB	0.3		1.0	1.6×10^{-2}*	1.0
A	1.6	1.9		1.0	1.0	A	0.9	0.7		4.6×10^{-3}*	1.0
IPV	2.7	0.9	1.0		1.0	IPV	4.3	4.5	5.1		3.8×10^{-3}*
IBR	2.5	1.1	0.8	0.2		IBR	1.0	0.7	5.8×10^{-3}	5.2	
Zr	BF	RB	A	IPV	IBR	Cd	BF	RB	A	IPV	IBR
BF		1.0	1.0	5.6×10^{-4}*	0.4	BF		1.0	1.0	1.0	1.0
RB	0.8		1.0	3.2×10^{-3}*	0.8	RB	0.2		1.0	1.0	1.0
A	0.2	0.6		1.1×10^{-3}*	0.5	A	0.4	0.2		1.0	1.0
IPV	6.1	5.3	5.8		0.07	IPV	0.3	0.5	0.3		1.0
IBR	2.4	1.6	2.1	3.8		IBR	0.5	0.3	0.6	0.8	
Ba	BF	RB	A	IPV	IBR	Pb	BF	RB	A	IPV	IBR
BF		1.0	1.0	4.5×10^{-4}*	0.7	BF		0.5	0.2	3.7×10^{-3}*	2.9×10^{-3}*
RB	0.9		0.9	3.8×10^{-3}*	0.3	RB	2.3		1.0	0.2	0.2
A	0.1	1.1		3.1×10^{-4}*	0.8	A	3.1	0.8		0.5	0.5

Table 7 (continued)

IPV	6.1	5.2	6.3		3.9×10^{-6}*	IPV	5.2	2.9	2.2		1.0
IBR	1.8	2.7	1.7	8.0		IBR	5.3	3.0	2.2	1.1×10^{-3}	

Q of Tukey below the diagonal and *p* (similar) above the diagonal

BF Barra Funda, *RB* Rodeio Bonito, *A* Ametista, *IPV* Iraí-Ponte Velha, *IBR* Iraí-BR 386

*Differed significantly ($p < 0.05$)

performed by PAleontological STatistics software, version 3.08 (Hammer 2015). The Grubbs statistical test was performed by the software QuickCalcs outlier calculator (Graphpad Software 2018). Data such as mean, confidence interval, and coefficient of variation were obtained in spreadsheets of the Microsoft Excel program, and the software SciDAVis (Sourceforge 2018) was used for the construction of graphs.

Results and discussion

Quality of the analytical process

The analytical quality of the EDXRF in species quantification was established in a test with 30 data recovery of MRC Green River Shale sediment (SGR-1b) from the United States Geological Survey. Simultaneous quantification via the fundamental parameters method was performed with the equipment Shimadzu, model EDX-720. The EDXRF technique demonstrated to meet the application requirements, according to figures of analytical merit (INMETRO 2018; Silva et al. 2016), assuring the reliability of the results for Al_2O_3, SiO_2, P_2O_5, K_2O, CaO, TiO_2, Fe_2O_3, Cr, Mn, Co, Cu, Zn, Zr, Ba, Cd, and Pb, as shown in Table 3.

The results of Table 3 confirm the good accuracy of the EDXRF technique, with coefficient of variance less than 20%, acceptable for environmental samples, and recovery compatible with MRC concentrations, with recoveries varying between 94.8 and 105.7% (INMETRO 2018). In the Supplementary Material (Table 1S), we present the results of the Grubbs test for elimination of outliers from the data set and the Kolmogorov-Smirnov test, which confirmed the fit of the data set in the Gaussian model.

The general table of mean concentrations obtained in the EDXRF analyses of the certified reference material (SGR-1b sediment) is presented in Supplementary Material (Table 2S), together with the established analytical merit figures. The accuracy of the method EDRXF was assessed by the chi-square criterion ($p = 0.05$), presented in the Supplementary Material (Table 3S).

Mean concentrations of chemical species

The concentrations of the chemical species present in the samples composed of soils collected on the banks of the Várzea River (riparian forest) are presented in Table 4 and served as reference in the calculations of the indices of environmental quality of the sediments.

Table 4 shows good accuracy in the data collection, with a small variance in the batch, ensured by CV values (%). The concentrations of the chemical species in the sediment samples are presented in Table 5.

It is possible to evaluate in Table 5 the spatial variation of the chemical species according to the sampling points, as well as the temporal variation in the different sampling campaigns. It is possible to emphasize the variation of the mineral oxide TiO_2 (second campaign) and the elements Zn and Cu (first campaign), Ba (second campaign), and Mn and Ba (third campaign) in the Iraí-Ponte Velha (IPV) sampling point.

Statistical analysis data set of the samples

ANOVA (Table 6) was performed on the sample set of sediments of Rio de Várzea, in order to evaluate the dispersion in relation to the different sampling points ($p = 0.05$). ANOVA does not show significant differences for the oxides P_2O_5 and Fe_2O_3 and elements Co, Cu, and Cd. This reinforced the choice of Fe_2O_3 as a reference element due to its low variability.

The Tukey test (Table 7) was used to identify significant differences between the sampling points in relation to the chemical species for the collection points. The Tukey test showed differences in the concentrations of Al_2O_3, TiO_2, Zn, Zr, and Ba present in Iraí-Ponte Velha (IPV), output of the mining zone, in relation to the other

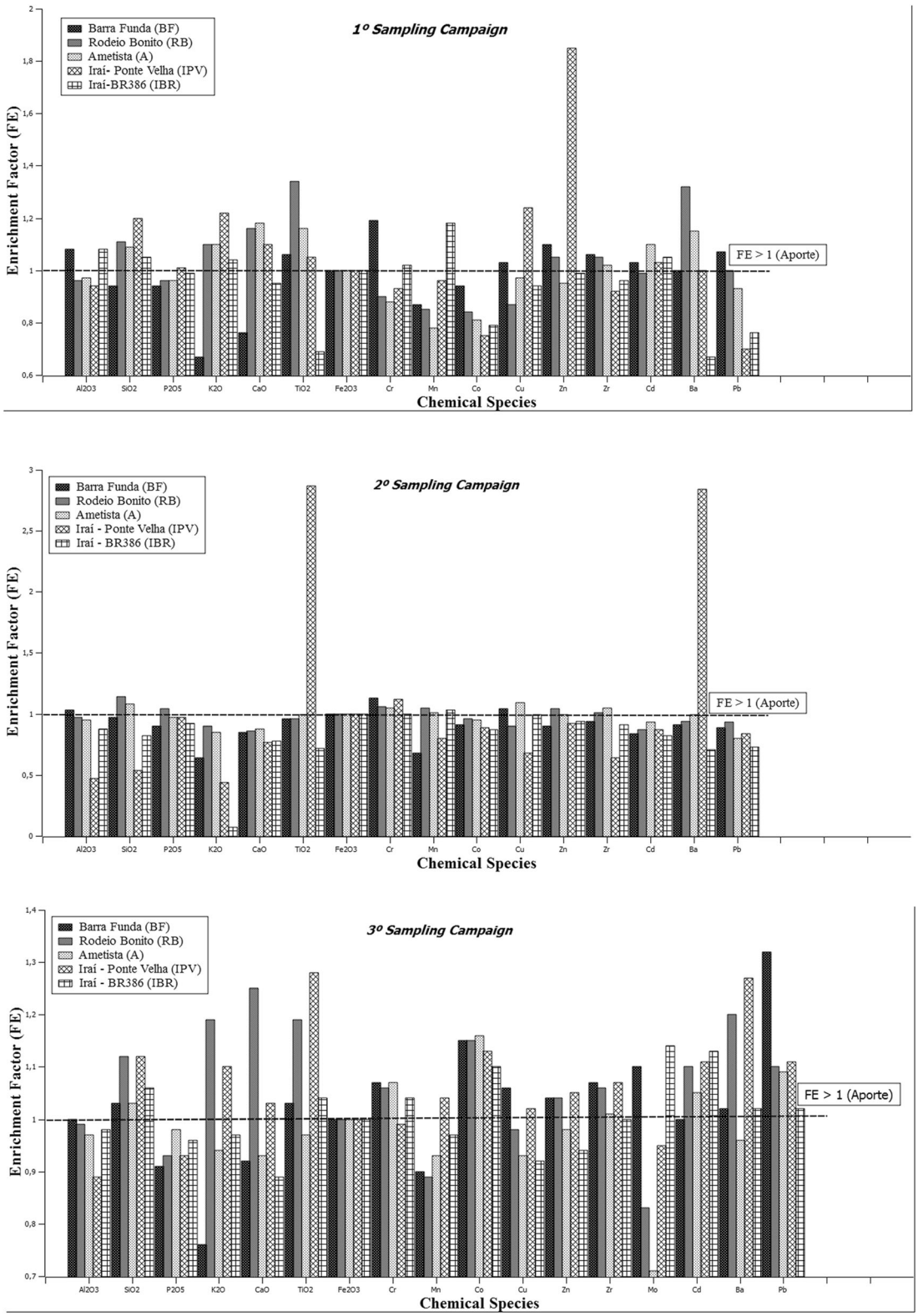

Fig. 4 Principal component analysis (PCA) considering the chemical species present in rocks, soils, and sediments

Table 8 Table of the PCA of the basalt rocks. Soil and sediment arrays—Várzea River

Summary			Forces		
MC	Eigenvalue	% variance	Analyte	MC1	MC2
1	38.0	75.0	Al_2O_3	− 0.01	0.8
2	4.1	8.0	SiO_2	− 0.1	0.3
3	2.7	5.3	P_2O_5	− 0.1	0.2
4	1.5	2.9	K_2O	− 0.1	0.1
5	1.1	2.1	CaO	− 0.1	0.07
6	0.9	1.8	TiO_2	− 0.002	0.1
7	0.7	1.4	Fe_2O_3	0.1	0.06
8	0.6	1.1	Cr	0.5	0.1
9	0.5	0.9	Mn	0.5	0.2
10	0.3	0.7	Co	0.1	0.01
11	0.1	0.3	Cu	− 0.03	− 0.1
12	0.1	0.2	Zn	0.3	0.3
13	0.1	0.1	Zr	− 0.1	0.08
14	0.04	0.07	Cd	0.4	− 0.08
15	0.02	0.04	Ba	0.1	− 0.08
16	0.003	0.005	Pb	0.2	0.07

MC main component, *MC1* MCA axis 1, *MC2* MCA axis 2

points. This fact reinforces the thesis that the activities of mineral extraction influence the quality of the sediments of River of Várzea, RS.

There were significant differences of Mn in the sampling point Iraí-BR386 (IBR), downstream of the mining zone, and CaO in the Barra Funda point (BF), upstream of the mining zone, in relation to the others, and from Pb to the same point in relation to IPV and IBR. It is believed that such differentiations are associated with agricultural activities and the contribution of urban effluents prior to and after the mining zone. The availability of Mn results from the combination of the pH, oxidation, organic matter, and equilibrium conditions with the Fe and Ca elements. Figure 4 shows the PCA result of crossing data of average concentrations of soils, rocks, and sediments.

Principal component analysis (PCA) was applied to the data set of EDXRF sediment and soil samples, as well as the concentrations found in basalt rocks (Table 1). In the PCA, we observed an approximation of the behavior of soil samples and sediment samples, both of which present a distance with respect to the behavior of basalt rocks as a function of Cr, Mn, Cd, Zn, Co, Ba, and Fe_2O_3 concentrations (axis 1–75.04%) and Al_2O_3, SiO_2, TiO_2, P_2O_5, K_2O, and Zr (axis 2–8.04%).

Also in Fig. 4, it is possible to observe the differentiation of the IPV sample point in relation to the other sediment collection points explained by the positive relations with Ba, Cu, and Zn concentrations and with negative relations with Al_2O_3, SiO_2, and TiO_2. The results of the PCA differentiate the sediment samples from the IPV sample point (exit of the mining zone) in relation to the others regarding the average concentration of the chemical species. This fact reinforces the hypothesis that the basalt tailings, from the mineral extraction process, are fragmented by inclement weather, are transported, and contribute to the river of Várzea, influencing the quality of its sediments.

Table 8 presents the explanations of the PCA axes according to their main components and the forces involved for all the chemical species of interest in this study. In Table 8, we observe the interaction forces that explain the influence of variance involved between axes 1 and 2 that explain more than 84% of the PCA data. With the PCA, we could find similarities and differences in the environmental factors and the average concentrations of the chemical species, in the different places of study.

Environmental quality indices

The calculation of the environmental quality indexes based on background strategies used as baseline soils of the riparian forests and allowed establishing the contamination factor (CF) and the geoaccumulation index (I_{Geo}) presented in Table 9.

Table 9 classifies the quality of sediments of Várzea River by CF as moderately contaminated with Cr, Zn, and Ba (point BF); SiO_2, K_2O, CaO, TiO_2, and Ba (RB); SiO_2, K_2O, CaO, TiO_2, and Ba (point A); SiO_2, K_2O, and Zn (point IPV); and Al_2O_3 and Mn (IBR point) during the first campaign. The FC in relation to the second campaign indicates moderate contamination for Al_2O_3 and Cr (point BF); SiO_2 (RB point); SiO_2 and Zr (point A); TiO_2, Mn, and Ba (IPV point); and Mn (IBR point). Also, Table 9 shows the moderately contaminated FC degree of the third campaign for Zr and Pb (point BF); SiO_2, K_2O, CaO, TiO_2, Ba, and Pb (RB); Cr and Pb (point A); SiO_2, K_2O, CaO, TiO_2, Zr, Ba, and Pb (IPV point); and SiO_2, CaO, and Cr (IBR point). I_{Geo} classified sediment pollution as unpolluted to moderately polluted with TiO_2, Ba, Zn (Point Iraí-Ponte Velha, exit

Table 9 Values of environmental quality indices (enrichment factor and geoaccumulation index) established for the Várzea River sampling points, southern Brazil

		BF		RB		A		IPV		IBR	
	Analyte	FC	I_{Geo}	CF	I_{Geo}	CF	I_{Geo}	CF	I_{Geo}	CF	I_{Geo}
1st sampling campaign	Al_2O_3	1.0	−0.5	0.9	−0.7	0.9	−0.6	0.9	−0.8	1.1	−0.5
	SiO_2	0.9	−0.7	1.1	−0.4	1.1	−0.5	1.1	−0.4	1.0	−0.5
	P_2O_5	0.9	−0.7	0.9	−0.7	0.9	−0.7	0.9	−0.7	1.0	−0.6
	K_2O	0.7	−1.3	1.1	−0.6	1.1	−0.6	1.1	−0.5	1.0	−0.7
	CaO	0.7	−1.0	1.1	−0.4	1.2	−0.4	1.0	−0.6	0.9	−0.7
	TiO_2	1.0	−0.5	1.3	−0.2	1.1	−0.4	1.0	−0.6	0.7	−1.1
	Fe_2O_3	1.0	−0.6	1.0	−0.6	1.0	−0.6	0.9	−0.7	1.0	−0.6
	Cr	1.2	−0.4	0.9	−0.8	0.9	−0.8	0.9	−0.8	1.0	−0.6
	Mn	0.8	−0.8	0.8	−0.8	0.8	−1.0	0.9	−0.7	1.2	−0.4
	Co	0.9	−0.7	0.8	−0.9	0.8	−0.9	0.7	−1.1	0.8	−0.9
	Cu	1.0	−0.4	0.8	−0.6	1.0	−0.5	1.2	−0.2	0.9	−0.5
	Zn	1.1	−0.5	0.9	−0.5	0.9	−0.7	1.7	0.2	1.0	−0.6
	Zr	1.0	−0.5	1.0	−0.5	1.0	−0.6	0.9	−0.8	0.9	−0.7
	Cd	1.0	−0.6	1.0	−0.6	1.0	−0.4	1.0	−0.6	1.0	−0.5
	Ba	1.1	−0.5	1.3	−0.2	1.1	−0.4	0.9	−0.7	0.7	−1.2
	Pb	1.0	−0.5	1.0	−0.6	0.9	−0.7	0.7	−1.2	0.8	−1.0
2nd sampling campaign	Al_2O_3	1.1	−0.4	0.9	−0.7	1.0	−0.6	0.5	−1.6	0.9	−0.7
	SiO_2	1.0	−0.5	1.1	−0.5	1.1	−0.4	0.5	−1.4	0.8	−0.8
	P_2O_5	0.9	−0.7	1.0	−0.6	1.0	−0.6	1.0	−0.6	0.9	−0.7
	K_2O	0.7	−1.1	0.9	−0.9	0.9	−0.8	0.5	−1.7	0.1	−4.3
	CaO	0.9	−0.7	0.8	−0.9	0.9	−0.8	0.8	−0.9	0.8	−0.9
	TiO_2	1.0	−0.5	0.9	−0.7	1.0	−0.6	2.9	1.0	0.7	−1.0
	Fe_2O_3	1.1	−0.5	0.9	−0.7	1.0	−0.5	1.0	−0.5	1.0	−0.5
	Cr	1.2	−0.3	1.0	−0.6	1.1	−0.5	1.1	−0.4	1.0	−0.5
	Mn	0.7	−1.0	1.0	−0.6	1.0	−0.5	0.8	−0.9	1.1	−0.5
	Co	1.0	−0.6	0.9	0.7	1.0	−0.6	0.9	−0.7	0.9	−0.8
	Cu	1.0	−0.4	0.8	−0.7	1.0	−0.4	0.6	−1.1	0.9	−0.5
	Zn	0.9	−0.7	1.0	−0.6	1.0	−0.6	0.9	−0.7	1.0	−0.6
	Zr	1.0	−0.6	1.0	−0.6	1.1	−0.5	0.6	−1.2	0.9	−0.7
	Cd	0.9	−0.8	0.8	−0.9	0.9	−0.7	0.9	−0.8	0.8	−0.8
	Ba	1.0	−0.6	0.9	−0.7	1.0	−0.6	2.9	1.0	0.7	−1.0
	Pb	0.9	−0.7	0.9	−0.8	0.8	−0.9	0.8	−0.8	0.7	−1.0
3rd sampling campaign	Al_2O_3	1.0	−0.6	1.0	−0.6	1.0	−0.6	0.9	−0.8	1.0	−0.6
	SiO_2	1.0	−0.5	1.1	−0.5	1.0	−0.6	1.1	−0.4	1.1	−0.5
	P_2O_5	0.9	−0.7	0.9	−0.7	1.0	−0.6	0.9	−0.7	1.0	−0.6
	K_2O	0.8	−1.1	1.2	−0.5	0.9	−0.8	1.1	−0.6	1.0	−0.7
	CaO	0.9	−0.7	1.2	−0.3	0.9	−0.7	1.0	−0.6	0.9	−0.7
	TiO_2	1.0	−0.5	1.2	−0.4	1.0	−0.6	1.3	−0.2	1.1	−0.5
	Fe_2O_3	1.0	−0.6	1.0	−0.6	1.0	−0.6	1.0	−0.6	1.0	−0.6
	Cr	1.0	−0.5	1.0	−0.5	1.1	−0.5	1.0	−0.6	1.1	−0.5
	Mn	0.9	−0.7	0.9	−0.8	0.9	−0.7	1.0	−0.6	1.0	−0.6
	Co	1.2	−0.4	1.1	−0.4	1.2	−0.4	1.1	−0.4	1.0	−0.4

Table 9 (continued)

	BF		RB		A		IPV		IBR	
Analyte	FC	I_{Geo}	CF	I_{Geo}	CF	I_{Geo}	CF	I_{Geo}	CF	I_{Geo}
Cu	1.1	−0.3	1.0	−0.5	0.9	−0.5	1.0	−0.4	1.1	−0.5
Zn	1.0	−0.5	1.0	−0.6	1.0	−0.6	1.0	−0.5	0.9	−0.6
Zr	1.1	−0.5	1.0	−0.5	1.0	−0.6	1.1	−0.5	1.0	−0.6
Cd	1.0	−0.6	1.1	−0.5	1.0	−0.5	1.1	−0.4	1.2	−0.4
Ba	1.0	−0.5	1.2	−0.4	0.9	−0.6	1.3	−0.2	1.0	−0.5
Pb	1.3	−0.2	1.1	−0.5	1.1	−0.4	1.1	−0.4	1.0	−0.5

FC contamination factor, I_{Geo} geoaccumulation index, *BF* Barra Funda, *RB* Rodeio Bonito, *A* Ametista, *IPV* Iraí-Ponte Velha, *IBR* Iraí-BR 386

from the mining area), and Co (Rodeo Bonito Point (RB), entrance to the mining zone).

When comparing the average concentrations of the chemical species present in the basalt rocks (rejects) (Table 1) with the average concentrations present in the soil samples collected in the riparian forest (Table 4), we verified that the wastes present higher concentrations in relation to the soils for K_2O, SiO_2, TiO_2, CaO, Zn, and Zr, which could support the hypothesis of sediment enrichment by inorganic chemical species as a consequence of mineral extraction activities.

In Fig. 5, the enrichment factors (EF) for chemical species are presented in the different collection points in different campaigns. Figure 5 shows a trend of contribution of some analyzed chemical species, such as SiO_2, K_2O, TiO_2, CaO, Ba, Mn, and Zn. However, it is worth noting the proximity to the transition line of some chemical species in Fig. 5, which slightly exceeds the threshold FE > 1 (Tiwari et al. 2013), such as Al_2O_3, Cr, Co, and Zr. This situation does not necessarily imply an abnormal entry of elements into the water system, as these values may be reflecting uncertainties associated with the baseline taken as background.

Figure 5 shows the moderate enrichment of the sediment samples by SiO_2, K_2O, Mn, Cu, and Zn (sample point IPV, mining zone) and TiO_2 and Ba (sample point RB, zone entry of mining). In the second sample campaign, the moderate sediment enrichment by TiO_2 and Ba (sampling point IPV, mining zone) can be highlighted. The third sample campaign highlights the moderate enrichment of the sediment samples by the Cr, Co, Mo, and Pb chemical species (sample point BF, upstream of the mining zone); SiO_2, K_2O, CaO, TiO_2, Co, Cd, Ba, and Pb (sample point RB, input of the mining zone); and SiO_2, K_2O, CaO, TiO_2, Co, Zn, Zr, Cd, and Ba of mining.

The FE values vary spatially and seasonally for different chemical species. This fact may be associated with the deposition and mining processes in the mining zone and the respective transport of fine sediments (< 63 μm) enriched due to hydrodynamic influences.

The sample points A (mining zone) and IPV (exit of the mining zone) are presented as moderately contaminated for the mineral oxides TiO_2, K_2O, SiO_2, CaO, and Al_2O_3 by the FC classification; FE indicates the contribution of these oxides, and the I_{Geo} classifies the points as moderately polluted for TiO_2. Pagnossin and Pires (2008), point out the presence of large concentrations of silica (SiO_2) in the mineral rocks of the region, this being the main constituent element of the Geodesy of amethyst. The volcanic effluent associated with the hydrothermal event that gave rise to the region altered the concentrations in the rocks of the mineral oxides Al_2O_3, K_2O, and Fe_2O_3 (Wildner and Lopes 2010; Branco 2002).

However, the same studies consider the oxides TiO_2, P_2O_5, and MgO as mineral oxides and properties in the geochemical event (Pinto and Hartmman 2011; Hartmann et al. 2015, Baggio et al. 2015). The sample points A (mining zone) and IPV (exit of the mining zone) are presented as moderately contaminated by the trace elements Cr, Zn, Ba, Mn, Zr, and Pb by the classification of FC, the FE indicates the contribution of these oxides in the same sample points, and IGeo classifies the points as moderately polluted for Ba, Zr, and Co.

The volcanic effluent associated with the hydrothermal event that gave rise to the region altered the Rb, Ba,

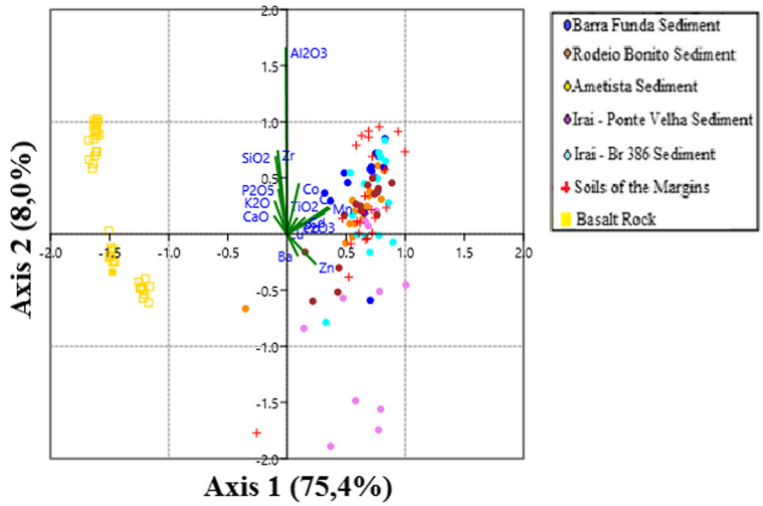

Fig. 5 Graph of the geochemical enrichment factor of the chemical species in relation to the sediment samples and taking as background the average concentrations present in soil samples from the riparian forest of Várzea River, southern Brazil

Sr, and Cu concentrations in the rocks. However, these same studies consider the oxides Zr, Th, Hf, Nb, Zr, and Ta as mineral oxides as immobile in the geochemical event (Hartmann et al. 2015; Baggio et al. 2015).

Conclusions

The mean concentrations of the mineral oxides Al_2O_3, SiO_2, P_2O_5, K_2O, CaO, TiO_2, and Fe_2O_3 and of the elements Cr, Mn, Co, Cu, Zn, Zr, Cd, Ba, and Pb and their possible deleterious effects on the environmental quality in river basins were investigated through soil samples from the ciliary woods and sediments of the Várzea River in southern Brazil. The study was developed in the mining region in the northern portion of the hydrographic basin where semiprecious rocks are extracted and where the municipality of Ametista do Sul is located which is the largest producer of amethyst rock in the world.

ANOVA showed the existence of significant differences between the campaigns and sample points ($p < 0.05$) for the chemical species Al_2O_3, SiO_2, K_2O, CaO, TiO_2, Cr, Mn, Zn, Zr, Ba, and Pb. Tukey's test showed differences ($p < 0.05$) for Al_2O_3, TiO_2, Zn, Zr, and Ba at the IPV point (exit of the mining zone), Mn at the IBR point, and CaO at the BF point in relation to the other sampling points.

The PCA differentiated sediments from the IPV point, leaving the mining zone, in relation to the others, reinforcing the hypothesis that the basalt tailings influence the sediment quality of Rio de Várzea, southern Brazil. The contamination factor (FC) classified the sediment samples as moderately contaminated in the sample campaigns for Al_2O_3, Cr, Zn, Ba, Cr, Zr, and Pb (point BF, upstream of the mining zone); SiO_2, K_2O, CaO, TiO_2, Ba, and Pb (point RB, entrance of the mining area); SiO_2, K_2O, CaO, TiO_2, Ba, Cr, Pb, and Zr (point A, mining zone); SiO_2, K_2O, CaO, TiO_2, Zn, Zr, Mn, and Ba (point IPV, exit of the mining zone); and Mn, SiO_2, CaO, Cu (Point IBR, upstream of the mining zone).

The use of I_{Geo} made it possible to evaluate the pollution of sediment samples indicating class 1 (non-polluted to moderately polluted) for TiO_2, Ba, Zn (point IPV, exit from the mining area), and Co (point RB, mining). The enrichment factor (FE) demonstrated the occurrence of chemical species due to anthropogenic mining activities, and classified sediment samples from Rio de Várzea as moderately enriched for SiO_2, K_2O, TiO_2, CaO, Mn, Cu, Zn, Zr, Ba, Co, and Cd (point PVI, exit of the mining zone), near the municipality of Ametista do Sul.

Nevertheless, the concentrations of chemical species and the environmental quality indices point to a moderate contamination of the area due to the mineral extraction activities, indicating a low possibility of occurrence of adverse effects to biota.

Acknowledgments The authors would like to thank Professor Cristiano Poleto of the Hydraulic Research Institute of UFRGS

and the journalist Andreia Primaz Eckhadt of the company O_2 Multicomunicações. Thanks also to the Federal University of Santa Maria (UFSM) as well as for the support of the National Council for Scientific and Technological Development (CNPQ) in the financing of research actions.

References

Ayari, J., Agnan, Y., & Charef, A. (2016). Spatial assessment and source identification of trace metal pollution in stream sediments of Oued El Maadene basin, northern Tunisia. *Environmental Monitoring and Assessment, 188*, 188–397.

Baggio, S. B., Hartmann, L. A., Massonne, H. J., Theye, T., & Antunes, L. M. (2015). Silica gossan as a prospective guide for amethyst geode deposits in the Ametista do Sulmining district, Paraná volcanic province, southern Brazil. *Journal of Geochemical Exploration, 159*, 213–226.

Branco, P. M. (2002). *Mapa gemológico do estado do Rio Grande do Sul*. Porto Alegre: CRPM - Serviço Geológico do Brasil (In Portuguese).

Canadian Council of Ministers of the Environment (CCME) (1995) Canadian sediment quality guidelines for the protection of aquatic life (EPC-98E Protocol for the derivation).

Enpresa Brasileira de Pesquisa Agropecuária (EMBRAPA) 2013. Sistema Brasileiro de Classificação de Solos, 3° edição, 20 p.

Esteves, F. A., & Camargo, A. F. M. (2011). *Sedimento Límnicos* (pp. 339–354). Rio de Janeiro: Editora Interciência.

Fan, W., Xu, Z., & Wang, W. (2014). Metal pollution in a contaminated bay: relationship between metal geochemical fractionation in sediments and accumulation in a polychaete. *Environmental Pollution, 191*, 50–57.

Filizola, H. F., Gomes, M. A. F., & Souza, & M. D. (2006). Amostragem de solos. In *Manual de procedimentos de coleta de amostras em áreas agrícolas para análise da qualidade ambiental: solo, água e sedimentos* (pp. 25–36). Jaguariúna: EMBRAPA Meio Ambiente.

Folha Do Noroeste. 2019. Ametista do Sul apresenta crescimento de exportação de pedras. Accessed on January 18, 2019. Available in < https://www.folhadonoroeste.com.br/noticias/ametista-do-sulapresenta-crescimento-de-exportacao-de-pedras/>

Fundação Estadual de Proteção Ambiental (FEPAM). Bacia hidrográfica do rio da Várzea. Disponível em: < http://www.fepam.rs.gov.br/>. (February 20, 2018, in Portuguese).

Gadens-Marcon, G.T., Mendonça-Filho, J.G., Guerra-Sommer, M., Carvalho, M.A., Pires, E.F., & Hartmann, L.A. 2014. Relation between the sedimentary organic record and the climatic oscilations in the Holocene attested by palynofacies and organic geochemical analyses from a pond of altitude in southern Brazil. *Annals of the Brazilian Academy of Sciences, 86(3)*, 1077–1099.

Graphpad Software. Quick Calcs outlier calculator. Disponível em: <http://graphpad.com/quickcalcs/Grubbs1.cfm>. (january 8, 2018).

Hammer, ø (2015). Software paleontological statistics (Past), Version 3.08. Natural History Museum. University of Oslo, 2015.

Hanif, N., Eqani, S. A. M. S., Ali, S. M., Cincinelli, A., Ali, N., Katsoyiannis, I. A., Trannver, Z. I., & Bokhari, H. (2016). Geo-accumulation and enrichment of trace metals in sediments and their associated risks in the Chenab River, Pakistan. *Journal of Geochemical Exploration, 165*, 62–70.

Hartmann, L. A., Medeiros, J. N. T., Baggio, S. B., & Antunes, L. M. (2015). Controls on prolate and oblate geode geometries in the Veia Alta basalt flow, largest world producer of amethyst, Paraná volcanic province, Brazil. *Ore Geology Review, 66*, 243–251.

Hartmann, L. A., Pertille, J., & Duarte, L. C. (2017). Giant-geode endowment of tumuli in the Veia Alta flow, Ametista do Sul. *Journal of South American Earth Sciences, 77*, 51–57.

Herath, D., Pitawala, A., Gunatilake, J., & Iqbal, M. C. M. (2018). Using multiple methods to assess heavy metal pollution in an urban city. *Environmental Monitoring and Assessment, 190*(657), 657. https://doi.org/10.1007/s10661-018-7016-5.

Instituto Nacional de Metrologia, Qualidade e Tecnologia (INMETRO). (2018). *Orientação sobre Validação de Métodos Analíticos*. São Paulo: Coordenação Geral de Acreditação (In Portuguese).

Kämpf, N., Streck, E.V. 2010. Solos. Geodiversidade do Estado do Rio Grande do Sul. Porto Alegre: CRPM, p. 51-70.

Kontos, K. N., Foteinis, S., Paigniotaki, K., & Papadogiannakis, M. (2016). A robust X-ray fluorescence technique for multielemental analysis of solid samples. *Environmental Monitoring and Assessment, 188*, 120–130.

Lone, A. M., Achyuthan, H., Shah, R. A., & Sangode, S. J. (2018). Environmental magnetism and heavy metal assemblages in lake bottom sediments, Anchar Lake, Srinagar, NW Himalaya, India. *International Journal of Environmental Research. DOI, 12*, 489–502. https://doi.org/10.1007/s41742-018-0108-9.

Maanan, M., Saddik, M., Maanan, M., Chaibi, M., Assobhei, O., & Zourahah, B. (2015). Environmental and ecological risk assessment of heavy metals in sediments of Nador lagoon Morocco. *Ecological Indicators, 48*, 616–626.

Matschullat, J., Ottenstein, R., & Reimann, C. (2000). Geochimecal background - can we calculate it? *Journal of Environmental Geology, 39*(9), 990–1000.

Museu de Solos do Rio Grande do Sul (MSRS). 2019. Solos de Planalto: unidade de Passo fundo. Accessed on January 10, 2019. Available in <http://w3.ufsm.br/msrs/index.php/explore/solos/121-um-passo-fundo>

Ontiveros-Cuadras, J. F., Ruiz-Fernández, A. C., Sanchez-Cabeza, J. A., Pérez-Bernal, L. H., Preda, M., & Páez-Osuma, F. (2018). Mineralogical signatures and sources of recent sediment in a large tropical lake. *International Journal of Sediment Research, 33*, 183–190.

Pagnossin, E. M., & Pires, C. A. F. (2008). Silicose em Garimpeiros de Ametista do Sul, Brasil. *Hygeia - Revista Brasileira de Geografia Médica e da Saúde, 4*(7), 51–71.

Pascaud, G., Boussen, S., Soubrand, M., Joussein, E., Fondaneche, P., Abdeljaouad, S., & Bril, H. 2015. Particulate transport and risck assessment of Cd, Pb and Zn in wadi contaminated by runoff from mining wastes in carbonated semi-arid context. *Journal of Geochemical Exploration, Netherlands. 152*, 27–36.

Pejman, A., Bidhendi, G. N., Ardestani, M., Saeedi, M., & Baghvand, A. (2015). A new índex for assessing heavy metals contamination in sediments: a case study. *Ecological Indicators, 58*, 365–373.

Periotto, F., & Cielo Filho, R. (2014). A mata ciliar: conceituação, considerações sobre conservação, ecologia e recuperação. In *Bacias hidrográficas e recursos hídricos* (pp. 73–92). Rio de Janeiro: Editora Interciência.

Pinto, M. V., & Hartmann, L. A. (2011). Flow-by-flow chemical stratigraphy and evolution of thirteen Serra Geral group basalt flows from Vista Alegre, southernmost Brazil. *Annals of Brazilian Academy of Sciences, 83*, 425–440.

Remor, M. B., Sampaio, S. C., Rijk, S., Boas, M. A. V., Gotardo, J. T., Pinto, E. T., & Schardong, F. A. (2018). Sediment geochemistry of the urban Lake Paulo Gorski. *International Journal of Sediment Research, 33*, 406–414. https://doi.org/10.1016/j.ijsrc.2018.04.009.

Rodrigues, A. P. C., Castilhos, Z. C., Cesar, R. G., Almosny, N. R. P., Linde-Arias, A. R., & Bidone, E. D. (2011). *Avaliação de risco ecológico: conceitos básicos, metodologia e estudo de caso*. Rio de Janeiro: CETEM/MCT (In Portuguese).

Rosenstengel, L. M., & Hartmann, L. A. (2012). Geochemical stratigraphy of lavas and fault-block structures in the Ametista do Sul geode mining district, Paraná volcanic province, southern Brazil. *Ore Geology Reviews, 48*, 332–348.

Ryan, J. G., Shervais, J. W., Li, Y., Reagan, M. K., Li, H. Y., Godard, M., Kirchenbaur, M., Whattam, S. A., Pearce, J. A., Chapman, T., Nelson, W., Prytulak, J., Shimizu, K., & Petronotis, K. (2017). Application of a handheld X-ray fluorescence spectrometer for real-time, high-density quantitative analysis of drilled igneous rocks and sediments during IODP Expedition 352. *Chemical Geology, 451*, 55–66.

Secretária do Ambiente e do Desenvolvimento Sustentável (SEMA) (2012). Relatório anual sobre a situação dos recursos hídricos no Estado do Rio Grande do Sul. Porto Alegre : Governo do Estado do Rio Grande do Sul (In Portuguese).

Silva, P. R. B., Makara, C. N., Munaro, A. P., Schnitzler, D. C., Wastowski, A. D., & Poleto, C. (2016). Comparison of the analytical performance of EDXRF and FAAS techhiques in the determination of metal species concentrations using protocol 3050B (USEPA). *International Journal River Basin Management, 14*, 401–406.

Silva, P. R. B., Schnitzler, D., & Poleto, C. (2017a). *Avaliação da qualidade dos sedimentos por índices de qualidade ambiental: panorama em periódicos da área. Estudos Ambientais. Volume 1 (pp. 95–112)*. Rio de Janeiro: Editora Interciência.

Silva, P. P., Santos, L. T. S. O., & Jesus, T. B. (2017b). Assessment of heavy metal contamination in sub-tropical riverine sediments using geoaccumulation index. *Ecotoxicoloy and Environmental Contamination, Brasil, 12*(1), 1–9.

Sourceforge. Software de geração gráfica SciDAVis. Disponível em: <http://scidavis.sourceforge.net/>. (January 02, 2018).

Sundararajan, S., Khadanga, M. K., Kumar, J. P. P. J., Raghumaran, S., Vijaya, R., & Jena, B. K. (2017). Ecological risk assessment of trace metal accumulation in sediments of Veraval Harbor, Gujarat, Arabian Sea. *Marine Pollution Bulletin, 114*, 592–601.

Tiwari, M., Sahu, S. K., Brangare, R. C., Ajmal, P. Y., & Pandit, G. G. (2013). Depth profile of major and trace elements in estuarine core sediment using the EDXRF technique. *Applied Radiation and Isotopes, 80*, 78–83.

Vosoogh, A., Saeedi, M., & Lak, R. (2016). Heavy metals relationship with water and size-fractionated sediments in rivers using canonical correlation analysis (CCA) case study, rivers of south western Caspian Sea. Environmental Monitoring and Assessment, 188-603

Wildner, W., & Lopes, R. C. (2010). *Evolução Grológica: do paleoproterozoico ao recente* (pp. 15–34). CRPM: Geodiversidade do estado do Rio Grande do Sul. Porto Alegre.